Talanta 99 (2012) 409–414

Contents lists available at SciVerse ScienceDirect

Talanta

journal homepage: www.elsevier.com/locate/talanta

A novel β-Cyclodextrin-QDs optical biosensor for the determination of amantadine and its application in cell imaging

Xiangzhao Ai [a], Lu Niu [a], Yanyi Li [b], Fengping Yang [a], Xingguang Su [a,*]

[a] Department of Analytical Chemistry, College of Chemistry, Jilin University, Changchun 130012, PR China
[b] High School Attached to Northeast Normal University, Changchun 130021, PR China

ARTICLE INFO

Article history:
Received 8 March 2012
Received in revised form
31 May 2012
Accepted 31 May 2012
Available online 7 June 2012

Keywords:
Amantadine
Fluorescence resonance energy transfer
CdTe quantum dots
Pharmaceutical formulation

ABSTRACT

In this paper, a novel optical biosensor for amantadine (AD) determination has been constructed successfully based on the fluorescence resonance energy transfer (FRET) between water-soluble β-Cyclodextrin (β-CD)-functionalized CdTe quantum dots (QDs) and Rhodamine B (RB). RB could enter the cavity of β-CD by hydrophobic interaction, and the process of FRET between QDs and RB occurred. However, the process of FRET was switched off with the addition of AD, due to its larger hydrophobic association constant with β-CD than that of RB. The fluorescence intensity of CdTe QDs (donor) would increase gradually with the increasing concentration of AD, which shown a good linear relationship in the range of 1×10^{-5}–1.6×10^{-4} mol/L with a correlation coefficient $R^2=0.998$. We also obtained a satisfactory result using this spectrophotometric method for the determination of AD in pharmaceutical formulation. Furthermore, β-CD-functionalized CdTe QDs with AD in the cavity were incubated with target HepG2 cells and could be observed in the cytoplasm of cells. The β-CD-functionalized CdTe QDs could act as a visible biomarker for AD in cancer cells fluorescence imaging, which presents a potential application in biomedical field.

1. Introduction

As a new kind of fluorescent and semiconductor material, quantum dots (QDs) have got more and more attention in nanomaterial and bioanalytical fields in recent years, including solar cell [1], cell imaging [2], drug delivery [3], protein tracking [4] and cancer diagnoses [5]. Compared with traditional organic dyes, QDs have many unique properties that make them widely used in the development of optical biosensor. Firstly, they have enormous absorption extinction coefficients and high fluorescent quantum yields. They have broad excitation spectrum, narrow and size-tunable emission spectrum and large Stokes shift. QDs with different emission wavelengths can be excited at a single wavelength, enabling them applied in multiplexed experiments. Secondly, the resistance to photobleaching and high stability of QDs in biological environment enable their applications extend to biomedical field. With these outstanding properties, QDs have been widely applied as an excellent optical biomarker in biological fields. Ishihama et al. successfully observed the movement of individual mRNAs labeled by QDs in interchromatin regions of Cos7 cells [6]. Singh utilized biocompatible Fe_3O_4–ZnO core–shell magnetic quantum dots (M-QDs) for cancer imaging and therapy [7].

For the application of QDs in complex physiological environment, the methods for QDs modification was important [8–10]. Most molecules can link with QDs by covalent bond [11], hydrophobic interaction [12], electrostatic interaction [13] or chelation [14]. Different QDs modification methods not only have effect on the combination of QDs and biomolecule, but also lead distinct distribution of QDs in various organs in vivo [15–17]. Ballou et al. studied the effects of four kinds of amphiphilic polymer-coated QDs on mice after injection into their tail veins [15]. Deposition of four kinds of QDs was seen in the liver, spleen, born marrow, lymph nodes and other organs, depending on the various coatings used.

Cyclodextrins (CDs), as a well-known molecular host, have been used as an ideal functional molecule to modify the surface of QDs [18–20]. CDs are cyclic oligosaccharides that consist of six, seven, or eight glucopyranose units in α, β and γ forms, respectively [21]. The β-CD-functionalized QDs have been applied in biomedical field for their biocompatibility and chiral selectivity [22,23]. Zhao et al. synthesized QDs coated with β-CD and used them to deliver siRNA in live cells [23]. The results showed that the β-CD coupled to amino acids outlayers greatly improved the biocompatibility of QDs and endowed it with lower cytotoxicity even at very high concentration.

Amantadine (AD) is an antiviral agent used against infection with influenza A virus and Parkinsons disease [24,25]. Several analytical methods, such as high performance liquid chromatography (HPLC) [26–29], gas chromatography (GC) [30], capillary electrophoresis (CE)

* Corresponding author. Tel.: +86 431 85168352.
E-mail address: suxg@jlu.edu.cn (X. Su).

0039-9140/$ - see front matter © 2012 Elsevier B.V. All rights reserved.
http://dx.doi.org/10.1016/j.talanta.2012.05.072

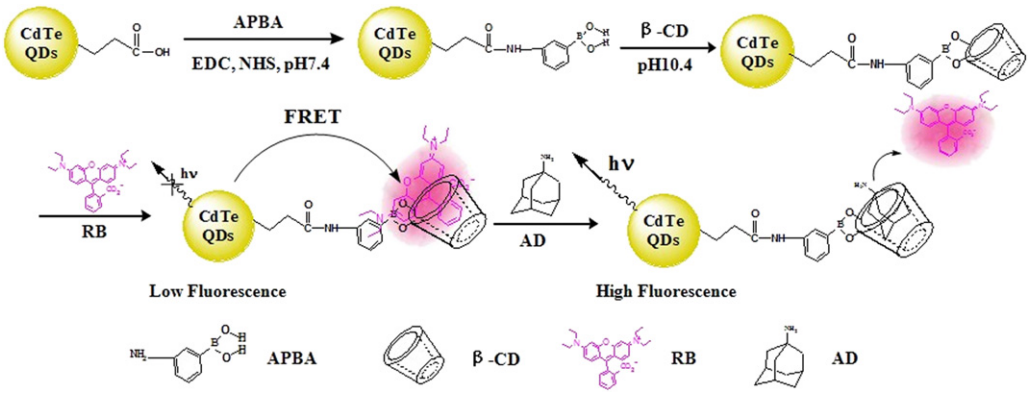

Scheme 1. Illustration of the optical biosensor for AD determination via FRET mechanism.

[31], have been reported for the determination of AD. Although some chromatographic methods have been the primary methods applied for the determination of the antiviral drugs in pharmaceutical formulations [27–29], however, the procedures are tedious, difficult to perform, and require more expensive apparatus, which could not be available in many laboratories. Spectrophotometric analysis is considered more convenient alternative technique because of its inherent simplicity and high sensitivity. However, few spectrophotometric methods have been reported for the determination of AD in pharmaceutical formulations, mainly due to that AD does not possess any chromophore in its molecule, which is essential for spectrophotometric methods. Therefore, derivatization [32] and formation complex with AD [33] were common ways before determination of AD by spectrophotometric methods. However, this process was laborious, time consuming, and not real time measurement. Therefore, it is significant to develop a simple, rapid, sensitive and non-derivative spectrophotometric method for AD determination. FRET as a fast, sensitive and non-destructive method has been widely used to develop various biosensors for the determination of bioactive molecules [34–37]. Freeman et al. reported a competitive optical sensing and chiral selective sensing for different substrates by using β-CD-functionalized CdSe/ZnS QDs, which was based on the fluorescence resonance energy transfer (FRET) or electron transfer (ET) mechanism [37]. This system combining QDs and β-CD not only has good selectivity and sensitivity, but also has excellent biocompatibility in vivo.

In this paper, we described a novel optical biosensor for amantadine determination based on FRET mechanism. We designed a FRET system by using water-soluble β-CD-functionalized CdTe QDs and Rhodamine B (RB). As shown in Scheme 1, RB could enter the cavity of β-CD by hydrophobic interaction and the process of FRET between QDs (donor) and RB (acceptor) occurred. When AD replaced RB in the cavity based on its larger hydrophobic association constant with β-CD, the process of FRET was switched off. We also obtained a satisfactory result using this method for the determination of AD in pharmaceutical formulations. Furthermore, β-CD-functionalized CdTe QDs with AD in the cavity were incubated with HepG2 cells and can be observed in cytoplasm by using fluorescence microscopy. The labeled QDs could reveal the location of AD in cells and this visible approach might offer a new visible biomarker for AD in cancer cells fluorescence imaging.

2. Materials and methods

2.1. Materials and reagents

All chemicals used were of analytical reagent grade without further purification. 3-mercaptopropyl acid (MPA), N-Hydroxysulfosuccinimide (sulfo-NHS) and 3-aminophenyl boronic acid (APBA) were purchased from J&K Chemical Co. Ltd. Tellurium powder, $CdCl_2$, $NaBH_4$ and 1-ethyl-3-(3-dimethylaminopropyl) carbodiimide hydrochloride (EDC) were purchased from Aldrich Chemical Co. Ltd. β-CD and Rhodamine B (RB) were purchased from Beijing DingGuo Biotechnology Co. Ltd. and AD was obtained from Dalian Meilun biotechnology Co. Ltd. respectively. Glucose, starch, vitamin C, sucrose, sodium citrate, cellulose and dextrin were purchased from Tianjin Guangfu Chemical Technology Co., Ltd. The pharmaceutical capsules were purchased from local drugstore. Dulbecco's modified Eagle's medium (DMEM) with high glucose was obtained from Invitrogen Co. and Fetal bovine serum (FBS) was purchased from Hyclone. 6-well plates were purchased from Corning Incorporated Co. The water used in all experiments had a resistivity higher than 18 MΩ/cm.

2.2. Instruments

Fluorescence experiments were performed on an RF-5301 PC spectrofluorophotometer (Shimadzu Co., Japan) and a 1 cm path-length quartz cuvette was used to measure the fluorescence spectrum. UV–vis absorption spectra were obtained using a GBC Cintra 10 e UV–vis spectrometer. The FT-IR spectrum was recorded on a Nicolet AVATAR 360 Fourier transform infrared spectrometer. Inverted fluorescence microscope (Olympus FV1000 IX71) equipped with a multispectral imaging system (Nuance, CRI, Woburn, MA, USA) was used to observe the location of β-CD-functionalized CdTe QDs in the cells.

2.3. Preparation of β-CD-functionalized CdTe QDs

CdTe QDs were synthesized by refluxing routes as described in detail in Ref. [38]. Briefly, the precursor solution of CdTe QDs was formed in water by adding fresh NaHTe solution to 1.25×10^{-3} mol/L N_2 saturated $CdCl_2$ solution at pH 11.4 in the presence of MPA as stabilizing agent. The molar ratio of Cd^{2+}/MPA/HTe^- was 1:2.4:0.5. The CdTe precursor solution was subjected to reflux at 100 °C under open-air conditions with condenser attached and different sizes of CdTe QDs were obtained at different refluxing times. The photoluminescence (PL) wavelength of CdTe QDs used in this study was 546 nm and the concentration of QDs was 1×10^{-6} mol/L.

β-CD-functionalized CdTe QDs were prepared by covalent link with APBA as a bridge. Briefly, 0.3 mL 2.5×10^{-6} mol/L EDC and 0.2 mL 1.5×10^{-6} mol/L sulfo-NHS were added into as-prepared QDs solution to activate carboxyl of QDs with stirring for 0.5 h. Then 0.5 mL 2.5×10^{-6} mol/L APBA solution was added and stirred for 3 h to form an amide bond between QDs and APBA. All the reactants above were prepared in 0.1 mol/L phosphate buffer solution (PBS, pH7.4). After adjusting the pH value from

7.4 to 10.4 by adding 100 μL 0.1 mol/L NaOH solutions, 0.5 mL 5×10^{-7} mol/L β-CD (dissolved in 0.1 mol/L PBS, pH10.4) was added into the reaction system with stirring overnight, and β-CD-functionalized CdTe QDs could be obtained.

2.4. Preparation of sample solution

Ten capsules were carefully evacuated; their contents were weighed and finely powdered. An accurately weighed quantity of the capsule contents equivalent to 100 mg of AD was transferred into a 100 mL calibrated flask, and dissolved in about 40 mL of distilled water. The contents of the flask were swirled, sonicated for 5.0 min, and then completed to volume with distilled water. The contents were mixed well and filtered rejecting the first portion of the filtrate. The prepared solution was diluted quantitatively with distilled water to obtain a suitable concentration for the determination of AD.

2.5. Cell imaging

The HepG2 cells were incubated in DMEM containing 10% heat-inactivated FBS at 37 °C in the humidified atmosphere with 5% CO_2 as described in Ref. [39]. For the β-CD-functionalized CdTe QDs staining, cells were seeded into a 6-well plate at a density of 3×10^5/well and incubated at 37 °C. When the cultured cells reached about 70% confluence, cells were incubated with β-CD-functionalized CdTe QDs at 37 °C for 12 h. After that, DMEM medium was taken out and we washed cells with PBS briefly. Then cells were fixed with 4% paraformaldehyde for 20 min and washed with PBS for at least three times. Fluorescent photos of the cell were taken by inverted fluorescence microscope equipped with Nuance system. All the image cubes were acquired using two multiple filters at 10 nm wavelength intervals with an automatic exposure time. Background and auto-fluorescence were removed from the final images.

3. Results and discussion

3.1. Absorption and emission spectrum of CdTe QDs and RB

As a well-known mechanism, the efficiency of FRET corresponds to the appreciable overlap between the emission spectrum of the donor and the absorption spectrum of the acceptor [40]. The more overlap, the higher efficiency of energy transfer. In this study, the appropriate size of CdTe QDs was chosen to maximize the overlap of the emission spectrum of QDs and absorption spectrum of RB. The absorption and fluorescence spectra of CdTe QDs and RB were shown (Fig. 1), respectively. It can be seen that the absorption spectrum of CdTe QDs was broad, and the maximal emission peak was at 546 nm. The maximal absorption and emission peaks of RB were at 564 nm and 581 nm, respectively. So there was appreciable overlap between the emission spectrum of the CdTe QDs (donor) and the absorption spectrum of the RB (acceptor).

3.2. FRET between CdTe QDs and RB

RB could enter the cavity of β-CD by hydrophobic interaction, and then the process of FRET between CdTe QDs and RB occurred. Fig. 2 displays the fluorescence spectra of this FRET system. It can be seen from Fig. 2 that the fluorescence emission intensity of CdTe QDs decreased while the fluorescence emission intensity of RB increased along with the addition of the RB concentration. This phenomenon indicated that FRET has occurred between donor and acceptor in solution. Moreover, the fluorescence emission

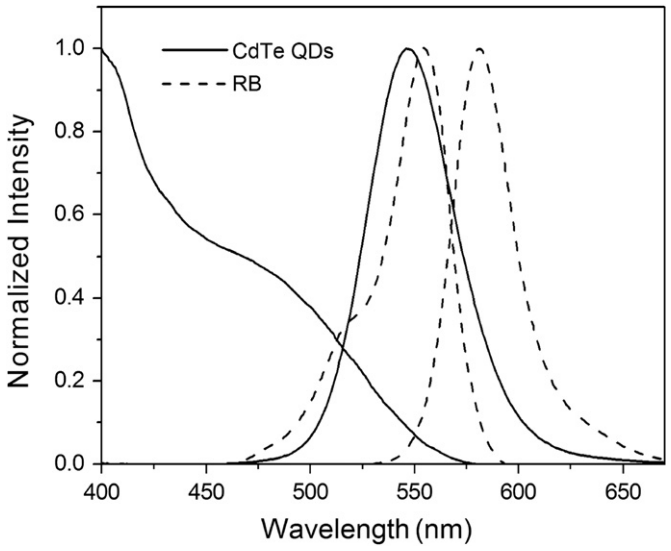

Fig. 1. Normalized absorption and emission spectrum of CdTe QDs and RB in solution.

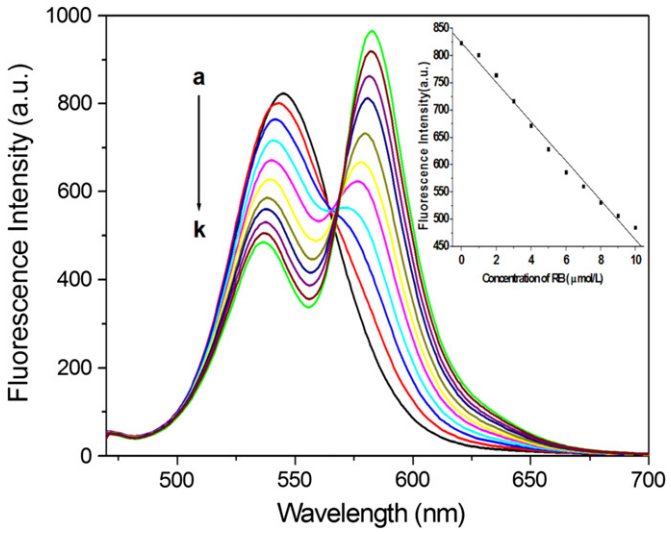

Fig. 2. Fluorescence spectra of FRET system with different concentration of RB. (a–k) Represents the concentration of RB of 0, 1×10^{-6} mol/L, 2×10^{-6} mol/L, 3×10^{-6} mol/L, 4×10^{-6} mol/L, 5×10^{-6} mol/L, 6×10^{-6} mol/L, 7×10^{-6} mol/L, 8×10^{-6} mol/L, 9×10^{-6} mol/L, 10×10^{-6} mol/L. The insert shows the linear relationship between the fluorescence intensity of CdTe QDs and the concentration of RB.

peaks of CdTe QDs blue-shifted from 546 nm to 537 nm, which resulted from the decrease of surface vacancies of CdTe QDs [41]. Meanwhile, the fluorescence emission peak of RB was red-shifted from 572 nm to 583 nm. The reason could attribute to the formation of dimer due to dipolar interaction between the RB molecules in water [42]. The insert shows the linear relationship between the fluorescence intensity of CdTe QDs and the concentration of RB. The linear regression equation was as follows: $F_{QDs}=823.52-36.13C_{RB}$ ($\times10^{-6}$ mol/L). The coefficient of correlation was $R^2=0.994$.

In this study, the energy transfer efficiency (E) was also calculated by Förster theory [40,43]. It is defined as the number of quanta transferred to the acceptor divided by the number of quanta absorbed by the donor. E can be measured experimentally and is commonly defined as

$$E=1-I/I_0 \quad (1)$$

where I and I_0 is the integrated fluorescence intensity of the donor in the presence and absence of the acceptor.

The relationship between energy transfer efficiency and the distance between the donor–acceptor pair is expressed as

$$E = R_0^6/(R_0^6+R^6) \quad (2)$$

where R is the real distance between donor–acceptor pair and R_0 is the critical distance between donor–acceptor pair at 50% energy transfers efficiency, which is calculated as follow equation:

$$R_0^6 = 8.8 \times 10^{-25} K^2 N^{-4} \phi J(\lambda) \quad (3)$$

where K^2 is the spatial orientation factor describing the relative orientation in the space of the transition dipoles of the donor and acceptor, N is the refraction index for the medium, φ is the fluorescence quantum yield of the donor in the absence of the acceptor and $J(\lambda)$ is the overlap integral between fluorescence emission spectrum of the donor and absorption spectrum of the acceptor. $J(\lambda)$ can be given by

$$J(\lambda) = [\Sigma I(\lambda)\varepsilon(\lambda)\lambda^4 \Delta\lambda]/[\Sigma I(\lambda)\Delta\lambda] \quad (4)$$

where $I(\lambda)$ is the fluorescence intensity of the fluorescence donor at wavelength λ, $\varepsilon(\lambda)$ is the molar absorption coefficient of the acceptor at wavelength λ and its unit is L/mol/cm. The overlap between the absorption spectrum of CdTe QDs and the fluorescence emission spectrum of RB is shown in Fig. 1. $J(\lambda)$ could therefore be calculated by Eq. (4) from the spectrum of FRET for λ=500–700 nm, and the value of $J(\lambda)$ is 1.047×10^{-10} cm^6/mol. Finally, we calculated that the distance (R) between QDs and RB was 5.28 nm. As known to us, the excitation energy of excited donor is nonradiatively transferred to a nearby acceptor via a through-space dipole–dipole interaction when the distance of donor and acceptor is in 1–10 nm [44]. This result fitted well with the estimated distance (5.24 nm) between the donor–acceptor pair in FRET system, which was calculated based on geometrical bonds lengths [37].

3.3. Optimize the ratio of β-CD/APBA

The concentration of β-CD is an important factor for AD determination, and only the RB that entered the cavity of β-CD could induce FRET process. In the present work, the effect of β-CD concentration on the FRET process was studied. The concentration of APBA was fixed and the concentration of β-CD was changed to get different ratio of β-CD/APBA. It can be seen from Fig. 3 that the decreasing extent of fluorescence intensity ($\Delta F = I_0 - I$) of CdTe QDs at 546 nm increased with the increasing ratio of β-CD/APBA up to 1:5. This could attribute to the increasing amount of β-CD-functionalized QDs with the increasing concentration of β-CD, which induces more FRET between QDs and RB. When the ratio of β-CD/APBA was higher than 1:5, the ΔF decreased. This phenomena could attribute to the reason that a part of RB molecular could enter the cavities of dissociative β-CDs by hydrophobic interaction when excess β-CDs exist in solution, so the amount of RB enter the cavities of β-CD-functionalized QDs would decrease, which resulted in less FRET between QDs and RB. Therefore, the ratio of β-CD/APBA of 1:5 was selected for further experiments.

In this study, the FT-IR spectrum was used to confirm that the β-CD had been linked to the surface of CdTe QDs. Fig. 4 shows the FT-IR spectra of CdTe QDs, β-CD and β-CD-CdTe QDs, respectively. The β-CD units were linked by the 3-aminophenyl boronic acid via the secondary vicinal hydroxyl groups of the sugar units [45]. It can be seen from Fig. 4 that the FT-IR spectrum of β-CD-CdTe QDs and β-CD showed a band at 1157 cm^{-1} which correspond to the asymmetric glycosidic vibration υ_a(C–O–C) and the bands at 1080 and 1030 cm^{-1} corresponding to the coupled stretch vibration υ(C–C/C–O). The band at 3400 cm^{-1} arises from the O–H

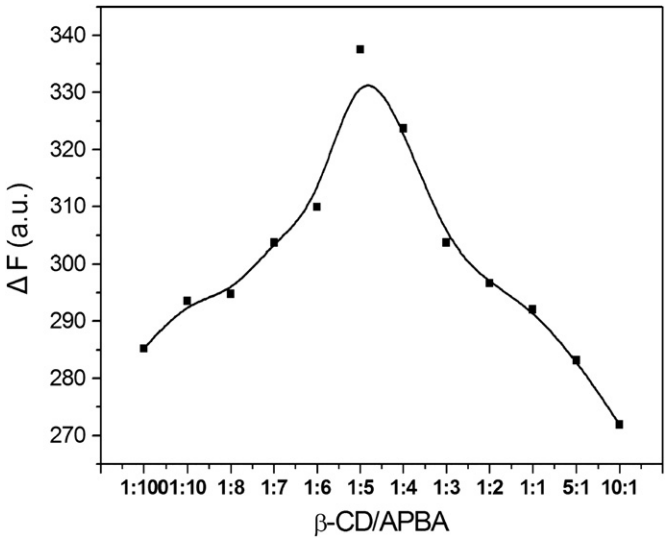

Fig. 3. Effect of β-CD/APBA ratio on the decreasing extent of fluorescence intensity ($\Delta F = I_0 - I$) of CdTe QDs at 546 nm. I_0 and I are the fluorescence intensity of β-CD-functionalized CdTe QDs in the absence and presence of RB in the FRET system.

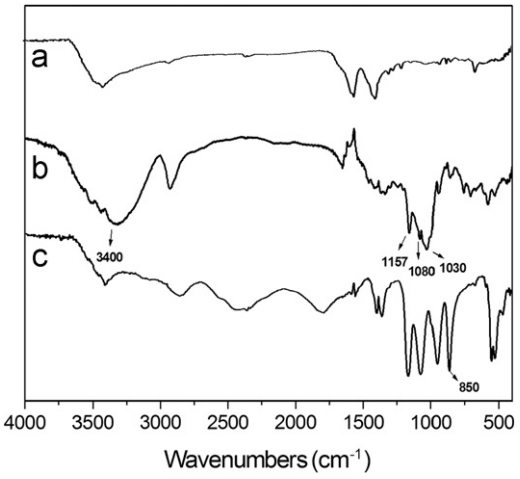

Fig. 4. FT-IR spectra of CdTe QDs (a), β-CD (b) and β-CD-CdTe QDs (c).

vibrations and the band at 850 cm^{-1} corresponds to the out-of-plane bending vibration γ(C–H). The FT-IR spectra confirmed that β-CD has been effectively linked to the surface of CdTe QDs.

3.4. Determination of AD with FRET system

When AD was added into the β-CD-functionalized QDs–RB system, AD would displace RB in the cavity of β-CD and then form 1:1 β-CD: AD inclusion complex. After a period of reaction time, dissociative RB and settled RB in the cavities of β-CD would achieve a state of equilibrium. This phenomenon could be proved by the recovery of fluorescence intensity of CdTe QDs in different incubation time. Fig. 5 shows the time-dependent fluorescence spectra of FRET system after the addition of AD. It can be seen that the fluorescence intensity of CdTe QDs gradually increased with the increasing of incubation time, and kept a constant intensity after an hour. Thus, we chose an hour as the optimal incubation time in further experiments.

In this study, AD can be determined with the established FRET system. As shown in Fig. 6, the fluorescence intensity of CdTe QDs at 546 nm increased gradually with the increasing concentration

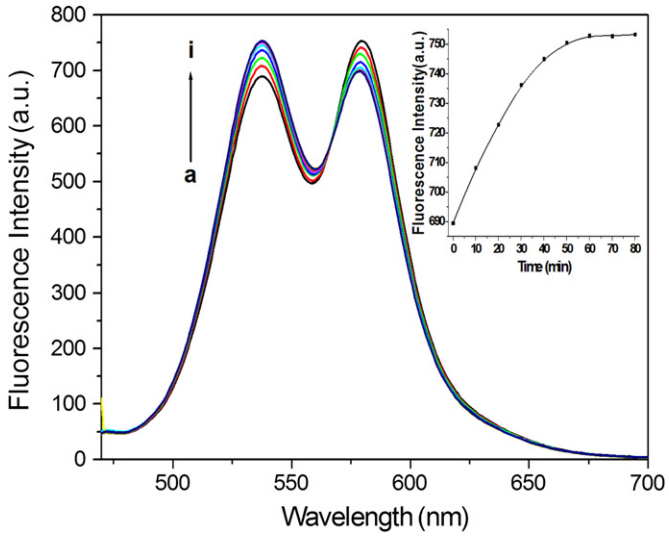

Fig. 5. Time-dependent fluorescence spectra of FRET system: (a) in the absence of AD and (b–i) in the presence of 2×10^{-4} mol/L AD. The inset shows the relationship between incubation time and the fluorescence intensity of CdTe QDs at 546 nm.

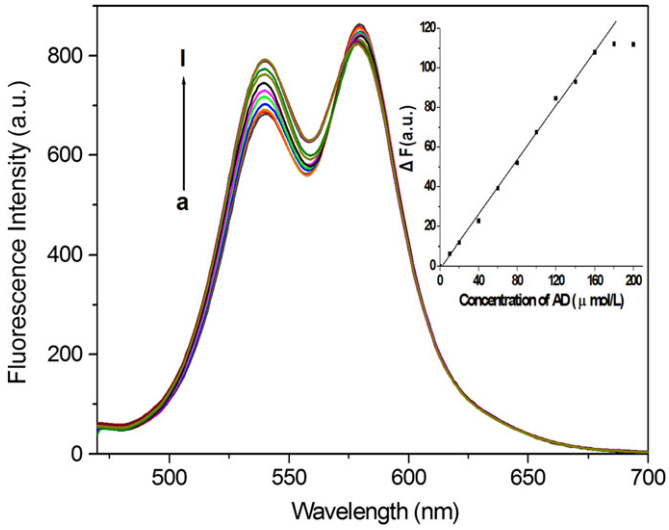

Fig. 6. Fluorescence spectra of the β-CD-CdTe QDs in the presence of AD at various concentrations. (a–l) Represents the concentration of AD of 0, 10×10^{-6} mol/L, 20×10^{-6} mol/L, 40×10^{-6} mol/L, 60×10^{-6} mol/L, 80×10^{-6} mol/L, 100×10^{-6} mol/L, 120×10^{-6} mol/L, 140×10^{-6} mol/L, 160×10^{-6} mol/L, 180×10^{-6} mol/L, 200×10^{-6} mol/L. The insert shows the relationship between the enhanced fluorescence intensity ($\Delta F=I-I_0$) of CdTe QDs at 546 nm and the concentration of AD.

of AD in the range of 1×10^{-5} to 2×10^{-4} mol/L. When the concentration of AD was higher than 1.6×10^{-4} mol/L, the fluorescence intensity of CdTe QDs almost achieved a flat. The insert in Fig. 6 displays the relationship between concentration of AD and the enhanced fluorescent intensity ($\Delta F=I-I_0$) of CdTe QDs. I_0 and I are the fluorescence intensity of β-CD-functionalized CdTe QDs in the absence and presence of AD in the FRET system. The linear regression equation was as follows: $\Delta F=0.69\times C_{AD}$ ($\times10^{-6}$ mol/L)-2.22, and the coefficient of correlation was $R^2=0.998$. The detection limit for AD was 8.82×10^{-6} mol/L.

3.5. Interference study

In this study, the selectivity of the established FRET system for AD detection was further evaluated with various coexistence substances added. Table 1 shows the interference effect of some common excipients in pharmaceutical dosage forms on the determination of AD, a relative error of $\pm5.0\%$ was considered to be tolerable. It can be seen in Table 1 that all the excipients in high concentration (≥100 fold of AD) do not have obvious effect on the determination of AD. The results indicated that there was little interference from common excipients in pharmaceutical dosage forms. Therefore, the β-Cyclodextrin-QDs optical biosensor can be used in the following direct determination of AD in pharmaceutical capsule.

Table 1
Interference of some common excipients in pharmaceutical dosage forms on the determination of AD (1.06×10^{-4} mol/L, 20 mg/L).

Coexisting substance	Concentration (mg/L)	$\Delta I^a/I$ (%)
Sucrose	10,000	0.87
Glucose	4000	−2.01
Starch	4000	−0.16
Vitamin C	2000	3.22
Sodium citrate	4000	−3.54
Cellulose	2000	−0.68
Dextrin	2000	−0.76

[a] $\Delta I=I-I_0$, where I_0 and I are the fluorescence intensity of CdTe QDs in the β-CD-functionalized CdTe QDs-AD FRET system in the absence and presence of coexisting substance.

Table 2
Results for the determination of AD in pharmaceutical capsule by the present spectrophotometric method.

Sample	Measured (mean ± SD, $n=3$)[a] (μmol/L)	Spiked (μmol/L)	Found (mean ± SD, $n=3$) (μmol/L)	Recovery (%)
Amantadine capsule	67.28 ± 0.73	40	40.24 ± 1.75	100.6
		80	79.26 ± 1.66	99.1
		120	120.16 ± 0.71	100.1

[a] Determined concentration of AD in pharmaceutical capsule after appropriate dilution (80-fold) of prepared pharmaceutical capsule sample solution in 100 mL flask.

3.6. Determination of AD in pharmaceutical capsule

In order to evaluate the accuracy, repeatability and selectivity of the present method, the established spectrophotometric method was used for the determination of AD in pharmaceutical capsule, and the results were shown in Table 2. The obtained mean value of content is calculated as 101.04 ± 1.83 mg per capsules, which is close to 100 mg labeled in leaflet of this medicine. The recovery of the spiked AD ranges from 99.1%–100.6%. The obtained satisfactory results made this spectrophotometric method suitable for the routine quality control analysis of AD in its dosage forms pharmaceutical formulation.

3.7. Fluorescence imaging of the HepG2 cells

In this study, the β-CD-functionalized CdTe QDs carried definite concentrations of AD were used to label the HepG2 cells. As shown in Fig. 7, the β-CD-functionalized CdTe QDs endocytosed by the cells were bright in fluorescence microscope imaging, which indicates that green β-CD-functionalized CdTe QDs with AD in the cavity of β-CD could permeate the cell membrane and distribute in the cytoplasm of cells. Moreover, the bright region in the graph indicated the location where drug delivery and release in the cells. Therefore, β-CD-CdTe QDs could act as

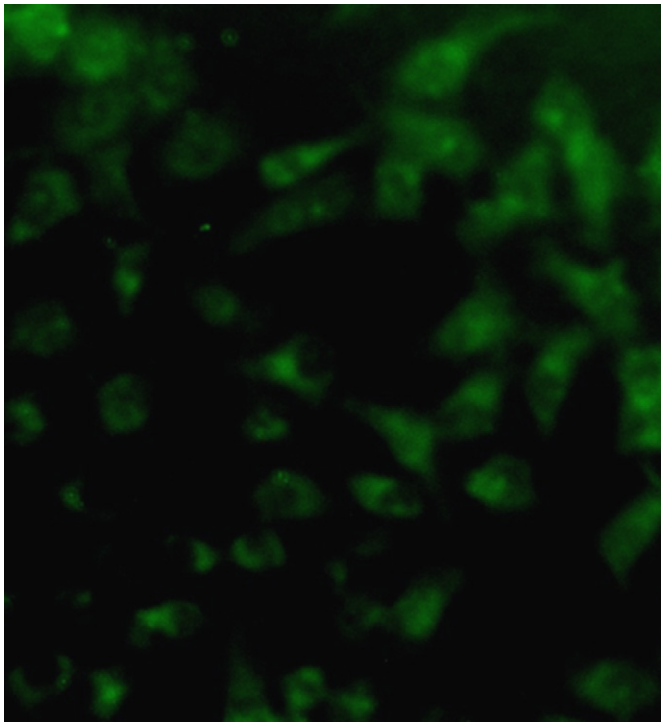

Fig. 7. Fluorescence imaging of HepG2 cells labeled with β-CD-functionalized QDs.

outstanding biomarkers for cancer cells fluorescence imaging which is under further investigations in our lab.

4. Conclusions

In this paper, water-soluble β-CD-functionalized CdTe QDs were prepared successfully. We applied this functionalized CdTe QDs to construct a sensitive optical biosensor for AD detection via FRET between CdTe QDs and RB, and also obtained satisfactory results using this spectrophotometric method for the determination of AD in pharmaceutical formulation. Furthermore, β-CD-functionalized CdTe QDs with AD in the cavity were incubated with targete HepG2 cells as a visible drug delivery carrier. The fluorescence imaging indicated that QDs labeled β-CD: AD inclusion complexes have distributed in the cytoplasm of cells. Nevertheless, there is still limitation of the present method, for instance, the selectivity of this method faces challenge when AD coexisting with some molecules which have similar structures with AD or parallel hydrophobic association constant with β-CD. However, it is feasible for AD determination in pharmaceutical formulations by this spectrophotometric method, which have been proved by the satisfactory results in this study. The present work not only provided a simple, rapid, sensitive and non-derivative spectrophotometric method for AD determination by FRET in pharmaceutical formulation, but also provides a visible biomarker for AD in cancer cells fluorescence imaging.

Acknowledgments

This work was financially supported by the National Natural Science Foundation of China (Nos. 20075009, 20875036, 21075050) and the Science and Technology Development Project of Jilin Province, China (No. 20110334).

References

[1] A.J. Nozik, M.C. Beard, J.M. Luther, M. Law, R.J. Ellingson, J.C. Johnson, Chem. Rev. 110 (2010) 6873–6890.
[2] A.M. Smith, H.W. Duan, A.M. Mohs, S.M. Nie, Adv. Drug Deliver. Rev. 60 (2008) 1226–1240.
[3] P. Zrazhevskiy, M. Sena, X.H. Gao, Chem. Soc. Rev. 39 (2010) 4326–4354.
[4] C.J. You, S. Wilmes, O. Beutel, S. Löchte, Y. Podoplelowa, F. Roder, C. Richter, T. Seine, D. Schaible, G. Uzé, S. Clarke, F. Pinaud, M. Dahan, J. Piehler, Angew. Chem. Int. Ed. 49 (2010) 4108–4112.
[5] J. Liu, S.K. Lau, V.A. Varma, B.A. Kairdolf, S.M. Nie, Anal. Chem. 82 (2010) 6237–6243.
[6] Y. Ishihama, T. Funatsu, Biochem. Biophys. Res. Commun. 381 (2009) 33–38.
[7] S.P. Singh, J. Biomed. Nanotechnol. 7 (2011) 95–97.
[8] A. Aboulaich, L. Balan, J. Ghanbaja, G. Medjandi, C. Merlin, R. Schneider, Chem. Mater. 23 (2011) 3706–3713.
[9] B. Pérez-López, A. Merkoci, Anal. Bioanal. Chem. 399 (2011) 1577–1590.
[10] A.J. Tavares, L.R. Chong, E. Petryayeva, W.R. Algar, U.J. Krull, Anal. Bioanal. Chem. 399 (2011) 2331–2342.
[11] R.S. Chouhan, A.C. Vinayaka, M.S. Thakur, Anal. Bioanal. Chem. 397 (2010) 1467–1475.
[12] C.P. Han, H.B. Li, Small 4 (2008) 1344–1350.
[13] B. Ghosh, A.J. Pal, Phys. Chem. Chem. Phys. 13 (2011) 9194–9200.
[14] X.A. Liu, L.X. Cheng, J.P. Lei, H. Liu, H.X. Ju, Chem. Eur. J. 16 (2010) 10764–10770.
[15] B. Ballou, B.C. Lagerholm, L.A. Ernst, M.P. Bruchez, A.S. Waggoner, Bioconjugate Chem. 15 (2004) 79–86.
[16] M. Bottrill, M. Green, Chem. Commun. 47 (2011) 7039–7050.
[17] A. Hoshino, S. Hanada, K. Yamamoto, Arch. Toxicol. 85 (2011) 707–720.
[18] C.P. Han, H.B. Li, Chin. Chem. Lett. 19 (2008) 215–218.
[19] K. Palaniappan, S.A. Hackney, J. Liu, Chem. Commun. 40 (2004) 2704–2705.
[20] M.Y. Guo, M. Jiang, Macromol. Rapid Commun. 31 (2010) 1736–1739.
[21] T. Ogoshi, A. Harada, Sensors 8 (2008) 4961–4982.
[22] M.X. Zhao, Q. Xia, X.D. Feng, X.H. Zhu, Z.W. Mao, L.N. Ji, K. Wang, Biomaterials 31 (2010) 4401–4408.
[23] M.X. Zhao, J.M. Li, L.Y. Du, C.P. Tan, Q. Xia, Z.W. Mao, L.N. Ji, Chem. Eur. J. 17 (2011) 5170–5178.
[24] T.H. Maugh, Science 206 (1979) 1058–1060.
[25] C. Paci, A. Thomas, M. Onofrj, Neurol. Sci. 22 (2001) 75–76.
[26] S.J. Cui, F. Feng, H. Liu, M. Ma, J. Pharm. Biomed. Anal. 44 (2007) 1100–1105.
[27] F.A.L. Van Der Horst, J. Teeuwsen, J.J.M. Holthuis, U.A.Th. Brinkman, J. Pharm. Biomed. Anal. 8 (1990) 799–804.
[28] P. Wang, Y.Z. Liang, B.M. Chen, N. Zhou, L.Z. Yi, Y. Yu, Z.B. Yi, J. Pharm. Biomed. Anal. 43 (2007) 1519–1525.
[29] T.H. Duh, H.L. Wu, C.W. Pan, H.S. Kou, J. Chromatogr. A 1088 (2005) 175–181.
[30] H.J. Leis, G. Fauler, W. Windischhofer, J. Mass Spectrom. 37 (2002) 477–480.
[31] H.H. Yeh, Y.H. Yang, S.H. Chen, Electrophoresis 31 (2010) 1903–1911.
[32] A.M. Mahmoud, N.Y. Khalil, I.A. Darwish, T. Aboul-Fadl, Int. J. Anal. Chem. (2009) 810104.
[33] H.A. Omara, A.S. Amin, Arab. J. Chem. 4 (2011) 287–292.
[34] A. Hillisch, M. Lorenz, S. Diekmann, Curr. Opin. Struct. Biol. 11 (2001) 201–207.
[35] D.L. Graham, P.N. Lowe, P.A. Chalk, Anal. Biochem. 296 (2001) 208–217.
[36] T.A. Perkins, D.E. Wolf, J. Godchild, Biochemistry 35 (1996) 16370–16377.
[37] R. Freeman, T. Finder, L. Bahshi, I. Willner, Nano Lett. 9 (2009) 2073–2076.
[38] X.Y. Wang, Q. Ma, B. Li, Y.B. Lin, X.G. Su, Luminescence 22 (2007) 1–8.
[39] M. Xue, X. Wang, H. Wang, B. Tang, Talanta 83 (2011) 1680–1686.
[40] Y.B. Li, Q. Ma, X.Y. Wang, X.G. Su, Luminescence 22 (2007) 60–66.
[41] T. Yu, J.S. Shen, H.H. Bai, L. Guo, J.J. Tang, Y.B. Jiang, J.W. Xie, Analyst 134 (2009) 2153–2157.
[42] S. Bakkialakshmi, T. Menaka, J. Mol. Liq. 158 (2011) 117–123.
[43] A.R. Clapp, I.L. Medintz, H. Mattoussi, Chem. Phys. Chem. 7 (2006) 47–57.
[44] D.M. Willard, L.L. Carillo, J. Jung, A.V. Orden, Nano Lett. 1 (2001) 469–474.
[45] C. Shimpuku, R. Ozawa, A. Sasaki, F. Sato, T. Hashimoto, A. Yamauchi, I. Suzukic, T. Hayashita, Chem. Commun. 13 (2009) 1709–1711.